Perturbing the High-Latitude Upper Ionosphere (F Region) with Powerful HF Radio Waves: A 25-Year Collaboration with EISCAT

N. F. Blagoveshchenskaya

Arctic and Antarctic Research Institute
38, Bering str.
St. Petersburg, 199397, Russia
E-mail: nataly@aari.nw.ru

Abstract

We present a brief review of experimental investigations concerning the perturbation of the high-latitude upper ionosphere (F region) by powerful HF radio waves (pump waves), carried out by the team from the Arctic and Antarctic Research Institute (AARI) during a 25-year collaboration with the European Incoherent Scatter (EISCAT) Scientific Association. Three types of HF pumping experiments were carried out by the Russian team at EISCAT. The first type of experiments was related to the modification of the ionosphere-magnetosphere coupling by HF pumping into the nightside ionosphere auroral E and F regions. The second type of experiments was concerned with investigations of geophysical phenomena by using the EISCAT HF heating facility and multi-instrument diagnostics. Most of the experiments were closely related to radio science and nonlinear plasma experiments (a third type of experiment). The main attention was paid to the investigation of artificial ionospheric turbulence in the upper ionosphere (F region) induced by the extraordinary (X-mode) HF pump waves. A great number of X-mode experiments, carried out by the Russian team at EISCAT, clearly demonstrated for the first time that an X-polarized HF pump wave was able to produce various HF-induced phenomena in the high-latitude ionospheric F region, which could be even much stronger than the O-mode effects. We found for the first time that the powerful X-mode HF radio waves, injected into the high-latitude ionospheric F2 layer towards the magnetic zenith, were capable of generating artificial field-aligned irregularities, radio-induced optical emissions in the red (630 nm) and green (557.7 nm) lines, strong electron acceleration leading to N_e enhancements, ion-acoustic and Langmuir electrostatic waves, and spectral components in the narrowband stimulated electromagnetic emission observed at a large distance from the HF heater. The features and behavior of the X-mode effects were analyzed and compared with the O-mode effects.

1. Introduction

The space environment forms a natural plasma laboratory for the investigation of various physical processes occurring in a plasma. In addition to naturally occurring phenomena, physical phenomena can be artificially excited by the injection of powerful radio waves (pump waves) into the ionosphere. Ionospheric-modification experiments by the use of ground-based high-frequency (HF) transmitters with high effective radiated power – so-called HF heating facilities – provide controlled detailed studies and understanding of various plasma processes in the ionosphere and magnetosphere. Such investigations are important for radio science, space weather, laser fusion, etc.

During 25 years, the team from the Arctic and Antarctic Research Institute (AARI), headed by me, collaborated with the EISCAT (European Incoherent Scatter) scientific association in conducting ionospheric modification experiments at Tromsø, with the use of the HF heating facility and the UHF incoherent-scatter radar (933 MHz). The largest number of experiments was carried out from 2008 to 2016 in the framework of the agreement between the EISCAT Scientific Association and AARI.

Three types of HF pumping experiments were carried out by the Russian team at EISCAT. The first type of experiment was related to the modification of the ionosphere-magnetosphere coupling by HF pumping into the nightside ionosphere auroral E and F regions towards the magnetic zenith (along the local geomagnetic field line) or near the magnetic field-aligned direction. The main attention here was paid to the search for distinctive features related to the modification of the ionosphere-magnetosphere coupling. We found evidence that HF pump waves injected into an auroral sporadic E layer were able to modify the natural auroral arc and to induce a local spiral-like formation [1-5]. Experimental results from multi-instrument observations

demonstrated that HF pumping into auroral E and F regions can lead to triggering of local auroral activation [1, 3, 5].

The intriguing evidence of the magnetospheric response to HF heater turn on and turn off was found from magnetic pulsation observations over a frequency range up to 5 Hz (the upper frequency limit of the sensitive magnetometer at Kilpisjarvi, located near Tromsø) [2]. The response manifested itself as spikes (main and echoing) in the dynamic frequency spectra. The main spikes were delayed in time by approximately 1 min after the HF heater turning on and off, and could be attributed to HF-induced Alfvén-wave pulses and their echoes seen in pulsation magnetometer data [2]. The ionospheric response to the HF heater turn on and off was presented in [6].

HF pumping into the F region is able to generate HF-induced ion upflows from the ionosphere, which were most pronounced in evening and night hours and were observed both under quiet [7, 8] and disturbed [2, 5] magnetic conditions. Different mechanisms responsible for the generation of ion upflows could be operating under quiet and disturbed background conditions.

The second type of experiments concerned investigations of geophysical phenomena by using the EISCAT HF heating facility and multi-instrument diagnostics [9-12]. The features of the magnetic pulsations in the *Pc*4-5 ranges were investigated in detail [10, 11]. An analysis of the experimental data obtained and numerical calculations demonstrated that depending on the level of the EISCAT/Heating facility power the observed wave activity in the *Pc*4 range was most probably induced by the intensification of natural stable *Pc*4 pulsations and by the generation of an Alfvén wave in a modified ionosphere [11].

We also showed that the combination of an HF-induced target and bistatic HF Doppler radio-scatter observations was a profitable method for probing medium-scale traveling ionospheric disturbances (TIDs) at high and mid-latitudes. HF ionospheric modification experiments provided a way of producing the HF-induced scatter target in a controlled manner at altitudes where the sensitivity to the TIDs was highest [12].

Most of the experiments carried out by the Russian team at Tromsø were closely related to the radio science and non-linear plasma experiments (the third type of experiment). As a general rule, HF pump waves with the ordinary polarization (O-mode) were used for the modification of the ionospheric F region. The ordinary-polarized HF pump waves interacted with the ionospheric plasma most efficiently at the reflection and upper-hybrid resonance altitudes. Nonlinear interaction between O-mode pump waves and the F-region ionospheric plasma produced a large number of phenomena that were successfully studied at all HF heating facilities in the world: see, for example, reviews [13-15] and references therein. The O-mode experiments, carried out by the Russian team, were focused to make up for some gaps in studies and understanding of HF-induced phenomena.

We found for the first time that the O-mode HF pump wave was capable of exciting the stimulated electromagnetic emission (SEE) near the second harmonic of the pump frequency [16]. The results obtained gave new and important information on the stimulated electromagnetic emission processes occurring in the downshifted maximum (DM) range of frequencies, and may guide us in the interpretation of these processes. This is a process that is very similar to that observed in the radio emission from the solar corona.

From multi-instrument observations in the course of an O-mode pumping experiment it was demonstrated that excitation of small-scale artificial field-aligned irregularities (AFAIs) is possible in the nightside auroral ionosphere [17].

The HF long-distance diagnostic tools located in St. Petersburg combined with multi-instrument observations at Tromsø were operated in conjunction with the ionospheric heating facility near Tromsø to examine the heater-induced phenomena in the auroral ionosphere during a magnetospheric substorm [18]. The procedure of ray-tracing simulation of the diagnostic HF signals scattered from artificial field-aligned irregularities was described in [19].

The aspect-angle dependence of O-mode HF pump-induced phenomena were analyzed from multi-instrument observations in the course of EISCAT heating experiments under quiet magnetic conditions. Experimental results revealed that the strongest electron temperature enhancements, optical emissions, and artificial field-aligned irregularities occurred when HF pumping was produced in the magnetic field-aligned pointing (magnetic zenith) direction [5, 7]. It was suggested that self-focusing of the HF pump wave on artificial field-aligned irregularities was a candidate mechanism for the magnetic zenith effect.

The properties of various HF-induced phenomena, such as artificial field-aligned irregularities, stimulated electromagnetic emission, optical emissions, Langmuir and ion-acoustic turbulence, strongly depend on the proximity of the pump frequency to the electron gyro-harmonic frequency (nf_{ce} , where n is the number of the harmonic and f_{ce} is an electron gyro-frequency). Features and behaviors of artificial field-aligned irregularities, stimulated electromagnetic emission, electron temperature and density, Langmuir and ion-acoustic plasma waves, seen from the incoherent-scatter radar as HF-induced plasma and ion lines, were analyzed in the course of pump-wave frequency stepping within 200 kHz of the nf_{ce} . Such investigations were made for third [20, 21], fourth [22], fifth, and sixth [23] electron gyro-harmonics. Distinctive features, possible generation mechanisms, and conditions of appearance of outshifted plasma lines were considered in [24].

In contrast to the O-mode HF pump wave, a powerful extraordinary (X-mode) HF radio wave did not match the

resonance altitudes because its reflection height was below the upper hybrid (UH) resonance altitude and the reflection altitude of the O-polarized pump wave. An X-mode HF pump wave should therefore not excite the thermal parametric (resonance) instability (TPI) responsible for the artificial field-aligned irregularity generation as well as the parametric decay instability (PDI), when it decays into electrostatic plasma waves such as a Langmuir wave (LW) and ion-acoustic wave (IAW). In addition, the electric field of the X-mode pump wave at the reflection altitude was perpendicular to the geomagnetic field, but the parametric decay instability excitation required a parallel electric field that was realized for the O-mode pump wave. However, a great number of X-mode experiments, carried out by the Russian team at EISCAT, clearly demonstrated for the first time that an X-polarized HF pump wave was able to produce various HF-induced phenomena in the high-latitude ionospheric F region that can be even much stronger than O-mode effects.

This review describes the various phenomena in the high-latitude ionospheric F region induced by X-mode HF pump waves and their comparison with the O-mode effects. Descriptions of the ionospheric modification experiments and diagnostic instruments are given in Section 2. Experimental results related to the distinctive features, behaviors, and possible generation mechanisms of small-scale artificial field-aligned irregularities (AFAIs), changes of plasma parameters (electron temperature and density, T_e and N_e), HF-induced optical emissions, Langmuir and ion-acoustic turbulence, and narrowband stimulated electromagnetic emission within ±1 kHz of the heater frequency are presented in Sections 3, 4, 5, 6, and 7, respectively. The results come from a large number of experiments carried out in day and evening hours under quiet magnetic conditions at different pump frequencies ($f_H = 4$ MHz to 8 MHz), lying below and above the critical frequency of the F2 layer. Concluding remarks and my thoughts concerning the future investigations of the X-mode effects are given in Section 8.

2. Description of Experiments and Diagnostic Instruments

Modification of the high-latitude ionospheric F region was produced by the EISCAT/heating facility near Tromsø in northern Norway (69.6°N, 19.2°E, magnetic dip angle $I = 77°$) [25]. HF pumping was produced by powerful X-mode polarized HF radio waves at frequencies below and above the critical frequency of the F2 layer ($f_H \le f_0F2$ and $f_H > f_0F2$). Alternating O-mode and X-mode HF pumping experiments were carried out under $f_H \le f_0F2$, when the O-mode and X-mode effects were possible. At low pump frequencies, in the range of 4 MHz to 5.5 MHz, phased array 2, with a beamwidth of 12° to 14° (at −3 dB level) and 22 dBi to 25 dBi gain was utilized. During the experiments, the effective radiated power (ERP) was 110 MW to 220 MW. At pump frequencies of 5.5 MHz to

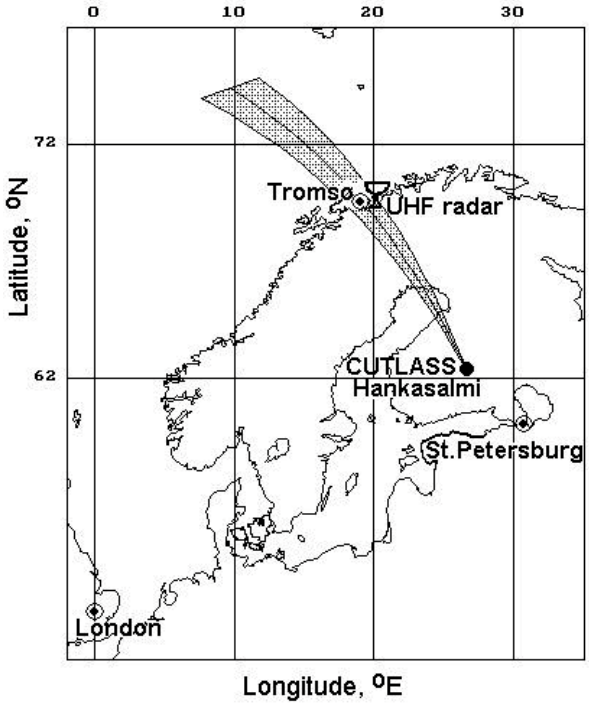

Figure 1. A map showing the location of the EISCAT/ heating facility, the EISCAT UHF incoherent-scatter radar, and the viewing geometry of the CUTLASS Hankasalmi (Finland) HF coherent scatter radar.

8 MHz, mostly phased array 1, having a narrow beamwidth of 5° to 6° and resulting in 28 dBi to 31 dBi gain, was used. In the course of experiments, the ERP was varied from 460 MW to 800 MW. Some experiments at frequencies of 5.5 MHz to 8 MHz were conducted by using phased array 3, with a wide beamwidth of 10° to 12° and 22 dBi to 25 dBi gain. In these experiments, the ERP was 130 MW to 240 MW. The HF heater beam was directed towards the magnetic zenith (12° south of vertical). However, for the investigation of the aspect-angle dependence, some experiments were carried out at three positions of the HF beam, such as 90° (vertical), 84°, and 78° (magnetic zenith). The transmission scheme of 10 min continuous wave (CW) on, 5 min off and 5 min on, 2.5 min off was most often used.

Multi-instrument diagnostics were used for the investigation of the X-mode HF-induced phenomena. The EISCAT UHF incoherent-scatter radar at 933 MHz [26], spatially collocated with the HF heating facility at Tromsø, was applied in the evaluation the ionospheric plasma parameters and HF-enhanced ion and plasma lines (HFILs and HFPLs) from the backscattered radar spectra. Artificial field-aligned irregularities were recognized from the backscattered signals received at Hankasalmi, Finland (62.3°N; 26.6°E) by the CUTLASS (Co-operative UK Twin Located Auroral Sounding System) HF coherent radar [27]. Observations were performed in a nonstandard mode, almost simultaneously at three frequencies from 10 MHz to 20 MHz, which allowed diagnostics of artificial field-aligned irregularities with spatial scales perpendicular to the magnetic field of 7.5 m to 15 m. HF-induced optical

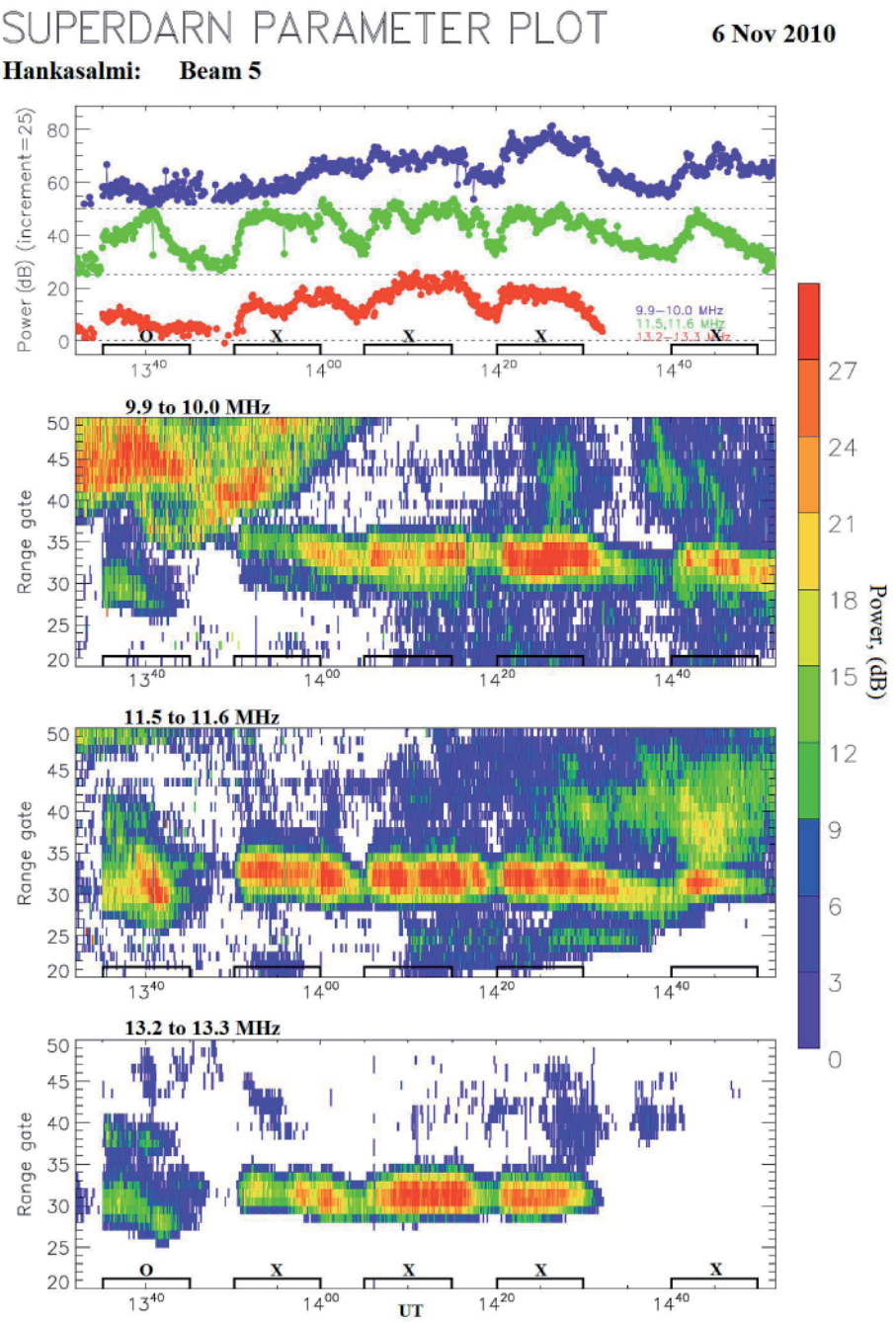

Figure 2. The backscattered power from the Hankasalmi (Finland) CUTLASS radar (beam 5) at operational frequencies of about 10 MHz, 11.5 MHz, and 13 MHz during the experiment on 6 November 2010 from 13:32 to 15:00 UT. The behavior of the backscattered power averaged between 30 to 34 gates, corresponding to the central part of the heated patch, is shown in the top panel and its behavior in the range-gate – universal-time UT coordinates is given in the bottom panels. The HF pump wave was radiated at a frequency of 4.544 MHz towards the magnetic zenith. The effective radiated power was about 180 MW. O/X-mode heater-on cycles are marked on the time axis (adapted from Blagoveshchenskaya et al. [33]).

emissions (artificial aurora) at red (630 nm) and green (557.7 nm) lines were observed at the Tromsø site by the Digital All-Sky Imager 2 (DASI-2) and from remote sites by the Auroral Large Imaging System (ALIS) [28] in Sweden. The observations of narrowband stimulated electromagnetic emission (NSEE) were conducted within ±1 kHz of the pump frequency in the vicinity of St. Petersburg (60°N, 30°E) at a distance from Tromsø of about 1200 km. Multi-channel HF Doppler equipment [29] near St. Petersburg and a net of oblique ionospheric sounders [30] were used for bi-static scatter observations of artificial field-aligned irregularities. The double-rhombic HF antenna system oriented to Tromsø was utilized in all measurements near St. Petersburg in the course of HF pumping experiments

for the narrowband stimulated electromagnetic emission (NSEE) observations. HF receivers for wideband stimulated electromagnetic emission (WSEE) measurements in the frequency band of 200 kHz were also employed at Tromsø. The status of the ionosphere in the course of experiments was checked by HF vertical sounders (Dynasonde and Digisonde) and magnetometers. The geometry of the experiments is shown in Figure 1.

3. Small-Scale Artificial Field-Aligned Irregularities (AFAIs)

Ionospheric modification experiments are providing the means for understanding mechanisms and physical processes leading to the generation and evolution of ionospheric irregularities. We present experimental results concentrating on the features and evolution, generation conditions and mechanisms of artificial field-aligned irregularities, with spatial scales across the geomagnetic field of 7.5 m to 15 m, in the high-latitude ionospheric F region induced by the controlled injection of the powerful HF radio waves from the ground into the ionosphere. The behavior and properties of artificial field-aligned irregularities excited by the O-mode HF pump waves are well known (see, for example, [13-15] and references therein). The main attention is paid to the recently discovered artificial field-aligned irregularities induced by the X-mode HF pump waves and their comparison with the O-mode artificial field-aligned irregularities [31-37].

A large number of experiments, carried out by the Russian team from 2010 to 2019 at EISCAT, clearly demonstrated that the X-mode HF pump wave was able to excite artificial field-aligned irregularities in the high-latitude ionospheric F region. In contrast to the O-mode, when artificial field-aligned irregularities were only generated under $f_H \le f_0F2$, the X-mode artificial field-aligned irregularities were excited in the course of HF pumping into the MZ at frequencies both below and above (up to 2 MHz) the critical frequency of the F2 layer ($f_H \le f_0F2$ and $f_H > f_0F2$) [21, 31, 33, 35, 37]. It is important to note that X-mode artificial field-aligned irregularities are generated in the regular *F* region under quiet conditions (no precipitation of particles, field-aligned currents, and electrojet).

Figure 2 presents the CUTLASS Hankasalmi backscatter power at three frequencies of ~10 MHz, 11.5 MHz, and 13 MHz, sensitive to artificial field-aligned

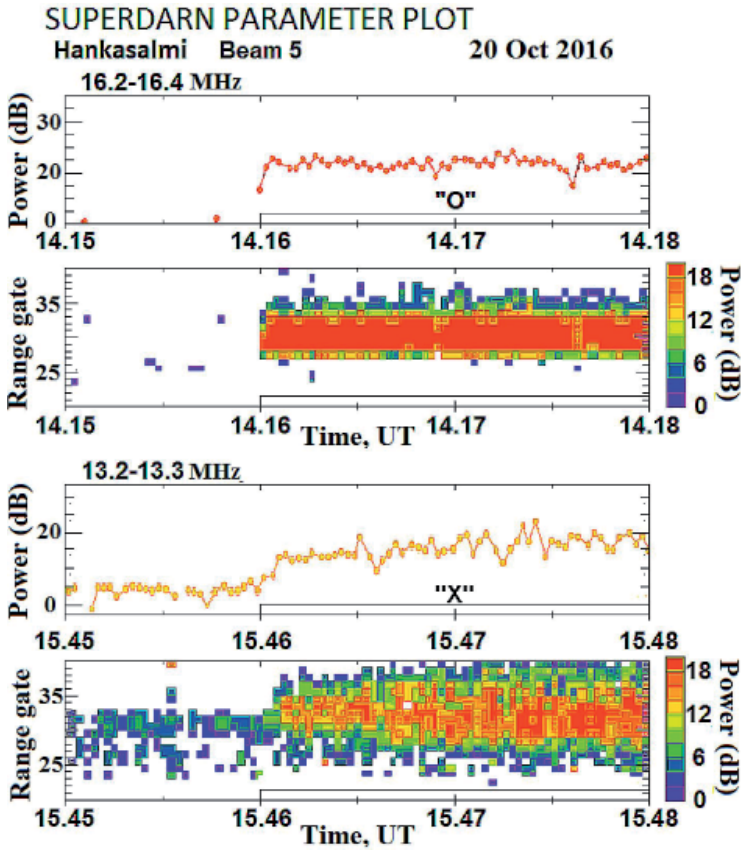

Figure 3. The backscattered power from the Hankasalmi (Finland) CUTLASS radar (beam 5) on 20 October 2016 for O-mode and X-mode heater pulses 1 min before the HF pumping onset and during the first 2 min of the heating cycles. The HF pump wave was radiated at a frequency of 4.544 MHz towards the magnetic zenith. The effective radiated power was about 130 MW. O/X-mode heater-on cycles are marked on the time axis (adapted from Blagoveshchenskaya et al. [32]).

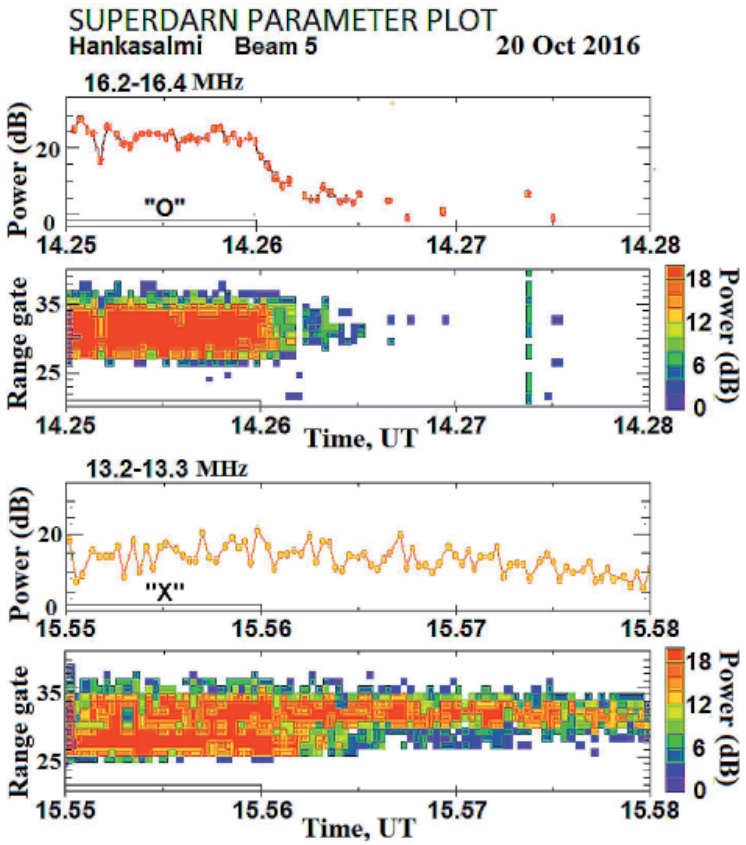

Figure 4. The backscattered power from the Hankasalmi (Finland) CUTLASS radar (beam 5) on 20 October 2016 for O-mode and X-mode heater pulses during the last minute of the heating cycles and the first 2 min after the HF heater was turned off. The HF pump wave was radiated at a frequency of 4.544 MHz towards the magnetic zenith. The effective radiated power was about 130 MW. The O/X-mode heater-on cycles are marked on the time axis (adapted from Blagoveshchenskaya et al. [32]).

irregularities with the spatial size across the geomagnetic field of the order of $l_\perp \approx 15$ m, 13 m, and 11 m, for a beam position centered on the Tromsø heater (beam 5) on 6 November 2010 [33]. HF pumping was produced towards the magnetic zenith at $f_H = 4.544$ MHz, which was above f_0F2.

The analysis of the entire volume of the CUTLASS data clearly demonstrated that the features and behaviors of the O-mode and X-mode artificial field-aligned irregularities radically differed. There was also a significant difference in the decay times for X-mode artificial field-aligned irregularities excited at high ($f_H = 5.5$ MHz to 8 MHz) and low ($f_H = 4$ MHz to 5.0 MHz) heater frequencies. The artificial field-aligned irregularity decay time at high pump frequencies did not exceed 3 min in the evening hours, whereas it can reach unusually long values exceeding the 5 min pause between the pump pulses at low heater frequencies.

Let us further compare the artificial field-aligned irregularity growth and decay times (t_1 and t_2) for O-mode and X-mode HF pumping. The CUTLASS backscatter powers, demonstrating the growth and decay times on 20 October 2016 ($f_H = 4.544$ MHz), are shown in Figures 3 and 4, respectively [37]. As seen, the artificial field-aligned irregularity growth and decay times significantly differed for O- and X-mode HF pumping. Upon the O-mode pumping, $t_1 = 6$ s to 9 s and $t_2 = 30$ s to 50 s. The growth and decay times for an X-mode pumping greatly depend on the preconditioning history. From a "cold" start (the first X-mode pulse), $t_1 \approx 60$ s to 70 s (it can even reach 150 s at $f_H > f_0F2$) and $t_2 \approx 100$ s to 130 s. In X-mode cycles with history, when the aftereffects of previous heating cycles act, t_1 decreased and t_2 increased [37].

It was found that the physical driving mechanisms of artificial field-aligned irregularities with a spatial scale across the geomagnetic field of 7.5 m to 15 m were significantly different for O-mode and X-mode HF pumping, presenting challenges for understanding the relevant processes. In contrast to the O-mode artificial field-aligned irregularities, excited by a thermal parametric (resonance) instability at the upper hybrid resonance altitude [13, 14],

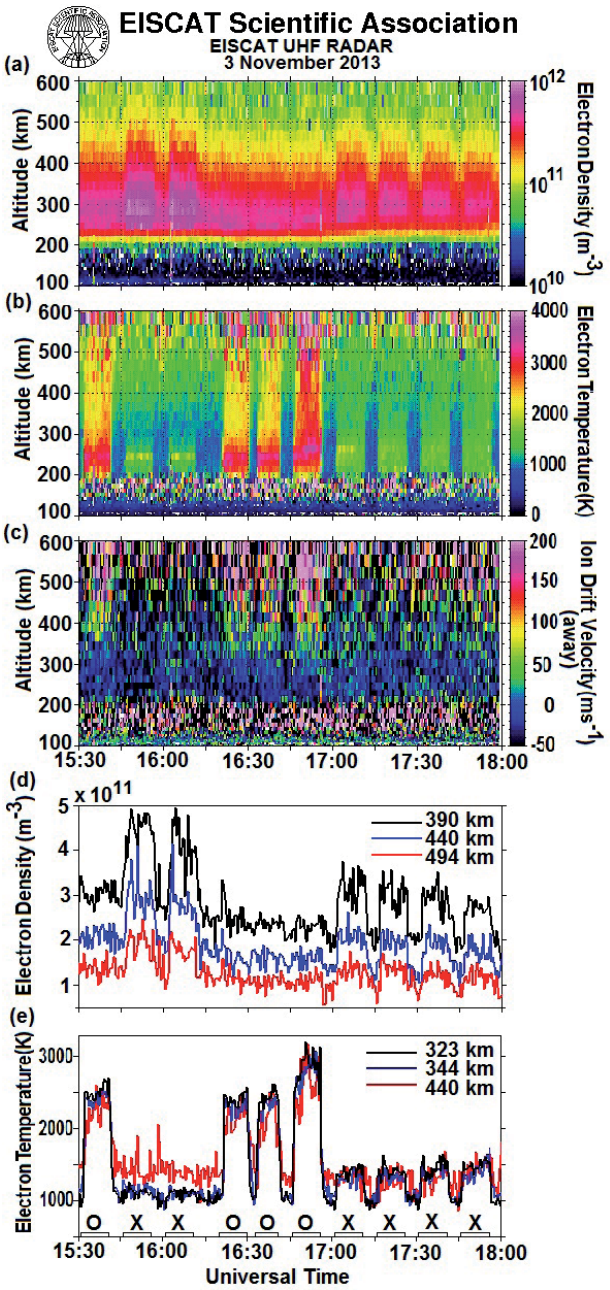

Figure 5. EISCAT UHF radar observations in the magnetic zenith (13°S) obtained with 30 s integration time during an HF modification experiment at Tromsø on 3 November 2013 from 15.30 to 18:00 UT. Altitude-temporal variations of the electron density (a), temperature (b), ion velocities (c), and variations in time at fixed altitudes of the electron density (d) and temperature (e) are shown. High-power HF radio waves with alternating O/X polarization were transmitted towards the magnetic zenith at a frequency of 6.2 MHz by pulses of 10 min on, 5 min off. The effective radiated power was about 450 MW. The heater pulses and polarization of the HF pump wave are drawn on the time axis of the bottom plot (adapted from Blagoveshchenskaya et al. [35]).

the X-mode artificial field-aligned irregularities were generated via a two-step process [31, 36-38]. In the first step, the generation of elongated large-scale irregularities (with a spatial scale across the geomagnetic field of the order of 1 km to 10 km) due to the self-focusing instability occurred. The excitation and behavior of small-scale artificial field-aligned irregularities was driven by large-scale irregularities. Their possible generation mechanisms could be the temperature-gradient-drift instability [38] or the filamentation instability [39].

4. Electron Density and Temperature Disturbances

We next consider the plasma parameter changes, such as the electron density and temperature (N_e and T_e), in the high-latitude ionospheric F2 layer induced by an X-mode HF pump wave. We compare them with the O-mode effects, depending on the ratio of f_H / f_0F2 .

Figure 5 depicts the altitude-temporal distribution of N_e, T_e, and ion velocities (V_i), as well as the N_e and T_e variations at fixed altitudes, from the EISCAT UHF radar observations on 3 November 2013 from 15:30 to 18:00 UT, when the critical frequencies f_0F2 gradually dropped from 6.7 MHz at 15:30 UT to 5.2 MHz at 18:00 UT [35]. In the course of the experiment, the HF pump wave radiated at $f_H = 6.2$ MHz towards the magnetic zenith with an effective radiated power of 450 MW. From 15:30 to 17:00 UT, when the pump frequency was below or near the critical frequency f_0F2 ($f_H / f_0F2 = 0.92 - 1.05$), alternating O/X pumping was carried out. From 17:00 UT, f_0F2 dropped to 5.8 MHz and excitation of the O-mode effects was made impossible because only X-mode HF pumping was performed.

As seen from Figure 5, large electron temperature increases, up to 2500 K to 3000 K (Figures 5b and 5e), accompanied by the generation of ion upflows from the ionosphere above ~350 km (Figure 5c), were observed under O-mode pumping. The electron-density changes were not significant. Such processes were a typical signature of the O-mode HF pumping, observed in previous EISCAT heating experiments [5, 7, 8, 40].

The opposite behavior (minor increases of electron temperature and large electron-density enhancements) was exhibited under X-mode HF pumping. Large electron-density increases of 50% to 70% were observed in a wide altitude range up to 600 km during all X-mode pump pulses (Figures 5a and 5d). Such N_e enhancements were a typical feature of X-mode pumping at different frequencies ($f_H = 4$ MHz to 8 MHz) but were most pronounced at high pump frequencies ($f_H = 6$ MHz to 8 MHz) from EISCAT UHF radar observations [31, 35, 36, 41]. These N_e enhancements occurred only in the magnetic field-aligned direction in a narrow-angle beam with a width of 3° to 4°around the magnetic field line [34, 35]. The N_e enhancements were accompanied by weak T_e increases (about 20% above the background values), when f_H was below the critical frequency ($f_H \le f_0F2$). However, the

T_e enhancements induced by ohmic heating increased up to 50% under $f_H > f_0F2$.

Strong N_e enhancements from EISCAT UHF radar measurements were common for X-mode pumping and were observed as often as the T_e enhancements under the action of O-polarized HF pump waves. They occurred along the magnetic field line in a wide altitude range whether or not the HF-enhanced ion and plasma lines were excited. The origin of large N_e enhancements, observed under X-mode HF pumping, is not yet understood, although one explanation involving ducting of the 933 MHz radar waves by field-aligned irregularities has recently been suggested [42]. However, we suggest that X-mode pumping towards the magnetic zenith initiates the acceleration of electrons, due to the fact that the electric field of a circularly polarized X-mode HF pump wave rotates in the same sense as the electron gyromotion. As was found in [43], the flux of accelerated electrons can produce an increased production of ionization. The presence of electron acceleration produced by the X-mode HF pumping towards the magnetic zenith is greatly confirmed by the optical observations. It was found that X-mode heating leads to a generation of very intense radio-induced optical emission in red and green lines with a high ratio of green to red line of 0.35 to 0.5 [34]. This experimental fact confirmed the presence of strong electron acceleration and therefore the enhanced electron density under X-mode pumping. One would expect that the duct of the enhanced electron density would guide the HF pump wave along the magnetic field line.

5. HF-Induced Optical Emission

We found from a set of repetitive experiments under quiet magnetic conditions that an X-polarized HF pump wave, radiated into the high-latitude ionospheric *F* region towards the magnetic zenith, can generate HF-induced optical emissions (HFOEs) at the red (630 nm) and green (557.7 nm) lines [34]. HF-induced optical emissions were generated at high pump frequencies ($f_H = 6.2$ MHz and 7.1 MHz), which were away from electron gyro-harmonics, under different ratios of the pump frequency f_H to f_0F2 ($f_H > f_0F2$, $f_H \approx f_0F2$, $f_H < f_0F2$). In the course of these experiments, the intensities of the red and green lines changed over a range of 110-950 R and 50-350 R, respectively. A comparison between the O- and X-mode HF-induced optical emissions clearly demonstrated the distinctions between them. The higher ratio of green to red line was typical for the X-mode HF-induced optical emissions. As shown in [34], the ratio of green to red lines for O-mode heating was $I_{577.7}/I_{630.0} = 0.22$ to 0.33, while under X-mode pumping this ratio reached the values of $I_{577.7}/I_{630.0} = 0.35$ to 0.5. Such high ratios of HF-induced optical emission intensities at green to red lines made it evident that strong electron acceleration was observed under X-mode pumping, which, in turn, can lead to the enhanced production of ionization along the magnetic field-aligned direction [43].

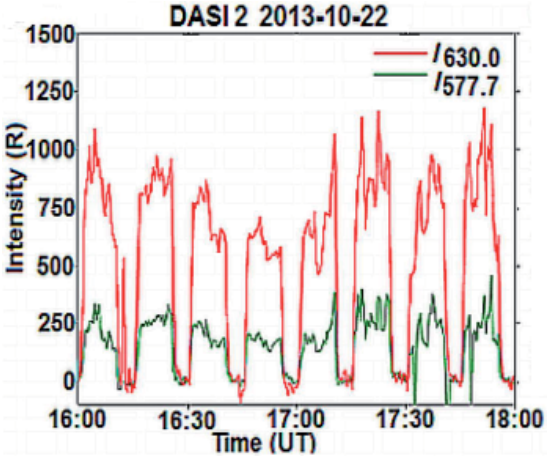

Figure 6. The intensity of the HF-induced optical emissions of the red (630.0 nm) and green (557.7 nm) lines imaged by the DASI-2 at the EISCAT site on 22 October 2013 from 16:00 to 18:00 UT. The X-mode pump wave was radiated at 7.1 MHz towards the magnetic zenith by 10 min on, 5 min off pulses beginning from 16:01 UT. In the course of the experiment, the effective radiated power varied between 458 MW to 548 MW (adapted from Blagoveshchenskaya et al. [34]).

Unusually intense X-mode emissions were excited on 22 October 2013, when they were simultaneously observed at the Tromsø site by DASI-2 and at the remote ALIS Abisko station. There the X-polarized continuous wave was radiated at 7.1 MHz using cycles of 10 min on, 5 min

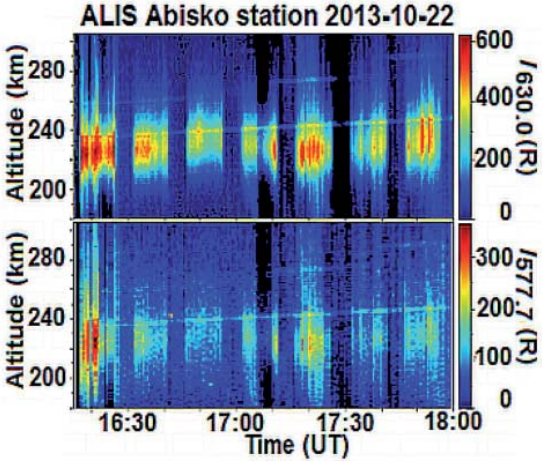

Figure 7. The altitude distribution of HF-induced optical emission intensities at red (630.0 nm) and green (557.7 nm) lines as a function of time (keogram) obtained at the ALIS Abisko station on 22 October 2013 from 16:00 to 18:00 UT. ALIS was looking at a volume above Tromsø and obtained one image every 10 s with an integration time of 6.5 s. The imager was running a filter sequence alternating between the emissions at 557.7 nm, 630.0 nm, and 844.6 nm. The X-mode pump wave was radiated at 7.1 MHz along the magnetic field by 10 min on, 5 min off pulses beginning from 16:01 UT. The effective radiated power varied between 458 MW to 548 MW (adapted from Blagoveshchenskaya et al. [34]).

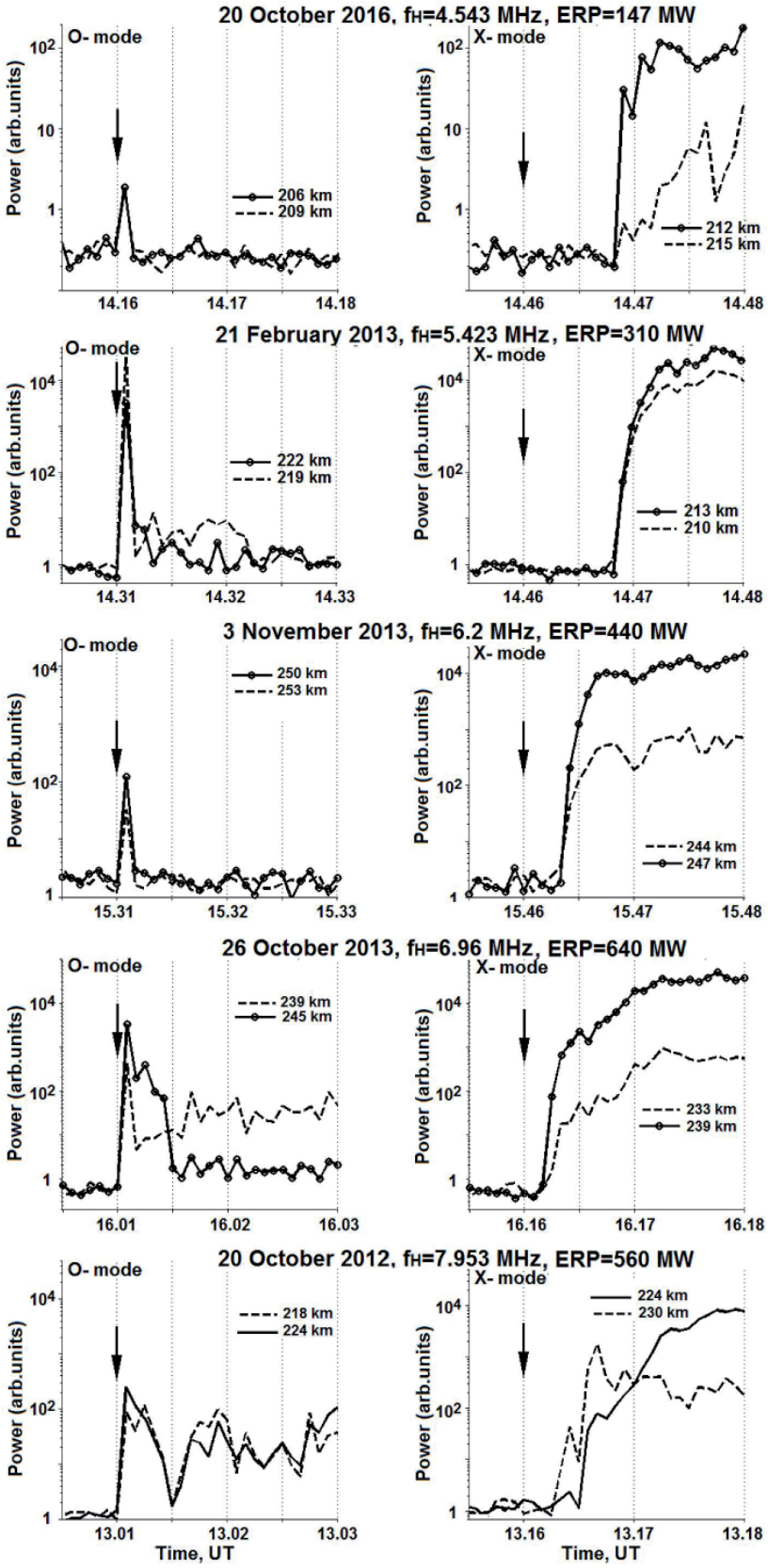

Figure 8. The temporal evolution of the power of HF-enhanced down-shifted plasma lines (HFPLs) with a 5 s resolution under O-mode and X-mode HF pumping at frequencies of 4.544 MHz, 5.423 MHz, 6.2 MHz, 6.96 MHz, and 7.953 MHz, 30 s before the HF pumping onset and during the first 2 min of the heating cycles. The HF-enhanced plasma line powers are shown at two fixed heights where they had maximum values (adapted from Blagoveshchenskaya et al. [36]).

off. The optical observations are shown in Figures 6 and 7 [34]. The intensity of HF-induced optical emissions of the red and green lines, taken by DASI-2 at the Tromsø site, is demonstrated in Figure 6. Strong artificial red and green line emissions, up to about 1000 R and 380 R above the background, respectively, were observed in every X-mode heater pulse from 16:00 to 18:00 UT. The DASI-2 camera was not able to determine the altitude structure of HF-induced optical emissions, but the ALIS camera at Abisco could do that. The altitude distribution of red and green line intensities as a function of time (keogram), taken from the ALIS Abisko station, is shown in Figure 7. As seen from Figure 7, the most intense radio-induced optical emissions were recorded in the altitude range of 215 km to 240 km. It is important that in the same altitude range the most intense HF-induced ion and plasma lines were excited in the EISCAT UHF radar measurements [34].

The distinctive feature of X-mode artificial optical emissions was their coexistence with the intense HF-enhanced ion and plasma lines, artificial field-aligned irregularities, and enhanced electron density in the magnetic field-aligned direction through the whole heater pulse. The O-mode HF-induced optical emission was accompanied by strong thermal electron heating and generation of ion upflows from the ionosphere [34].

6. Langmuir and Ion-Acoustic Turbulence

Incoherent-scatter radar collocated with the HF heater is capable of providing investigations of Langmuir (L) and ion-acoustic (IA) plasma waves. They are directly evidenced from radar spectra as HF-enhanced plasma (HFPL) and ion (HFIL) lines [44, 45].

We analyzed the distinctive features and behaviors of HF-enhanced Langmuir and ion-acoustic turbulences induced by the O-mode and X-mode HF pump waves radiated into the high-latitude ionospheric F region towards the magnetic zenith [36, 41, 46, 47]. Results came from a large number of alternating O/X-mode experiments carried out at the pump frequencies of f_H = 5.423 MHz; 6.2 MHz; 6.96 MHz; 7.1 MHz; 7.953 MHz with an ERP = 450 MW to 650 MW under quiet magnetic conditions. Note that X-mode HF-enhanced plasma lines and HF-enhanced ion lines were excited at pump frequencies both below and above f_0F2 ($f_H \le f_0F2$ and $f_H > f_0F2$). In the case $f_H > f_0F2$, HF-induced plasma and ion lines were generated in the frequency range between f_0F2 and f_xF2 , where f_xF2 is the critical frequency of the extraordinary component of the $F2$ layer ($f_xF2 = f_0F2 + f_{ce}/2$, where f_{ce} is the electron gyro-frequency) [35].

An essential difference in the temporal evolution of HF-enhanced plasma lines and HF-enhanced ion lines excited by O-mode and X-mode HF pump waves at frequencies $f_H \le f_0F2$ was found. Figure 8 demonstrates the temporal evolution of the maximum power of the HF-enhanced downshifted plasma line (HFPL) with a 5 s resolution under O-heating and X-heating at frequencies of 4.544 MHz, 5.423 MHz, 6.2 MHz, 6.96 MHz, and 7.953 MHz, 30 s before the HF pumping onset and during the first 2 min of the heating cycles [36]. The HF-enhanced plasma line powers are shown at two fixed heights where they had maximum values. The same behavior was also observed for HF-enhanced ion lines [41].

The O-mode pump onset was accompanied by the immediate increase of the plasma and ion line intensities observed in the first few 5 s dumps. That was a classic manifestation of the resonance parametric decay instability (PDI), when the powerful electromagnetic wave (pump wave) decays into Langmuir and ion acoustic plasma waves. Thereafter, the completely developed artificial field-aligned irregularities prevent any further parametric decay instability excitation. However, under high effective radiated power (ERP > 250 MW to 300 MW), preferably at high pump frequencies (f_H = 7 MHz to 8 MHz), the reappearance of HF-enhanced plasma lines and HF-enhanced ion lines can occur after the initial overshoot. They coexisted with artificial field-aligned irregularities, gradually enhanced, similar to the X-mode effects, but their intensity was much lower as compared to the intensity of the X-mode Langmuir and ion-acoustic waves (see Figure 8).

The appearance of the X-mode Langmuir and ion-acoustic plasma waves was delayed by 15 s to 30 s from the heating onset. Their intensity then smoothly enhanced and maximized within about 1 min, when artificial field-aligned irregularities were generated [41]. Such a behavior of HF-induced plasma and ion turbulence corresponded to the development of the non-resonance type instability in which artificial field-aligned irregularities played a key role. Coexisting HF-enhanced plasma and ion lines and artificial field-aligned irregularities during the whole pump pulse was a typical feature of X-mode experiments. It was also found that intense HF-enhanced plasma lines and HF-enhanced ion lines coexisted with the HF-induced optical emissions at red and green lines with high ratio of green to red lines [34].

It was shown that excitation thresholds for the parametric decay instability (PDI), represented in the radar spectra as HF-enhanced plasma and ion lines, significantly differed for the O-mode and X-mode HF pumping towards the magnetic zenith [41]. Results from a power stepping experiment at f_H = 7.953 MHz demonstrated that the X-mode parametric decay instability excitation threshold was 0.47 V/m. The O-mode persistent plasma and ion-line backscatters, coexisting with artificial field-aligned irregularities, showed an excitation threshold of 0.62 V/m, which exceeded the thresholds for the X-mode HF-enhanced plasma lines and HF-enhanced ion lines, while their intensity was two orders of magnitude less [41]. For the same background conditions and pump frequency, the "classic" resonance parametric decay instability, excited

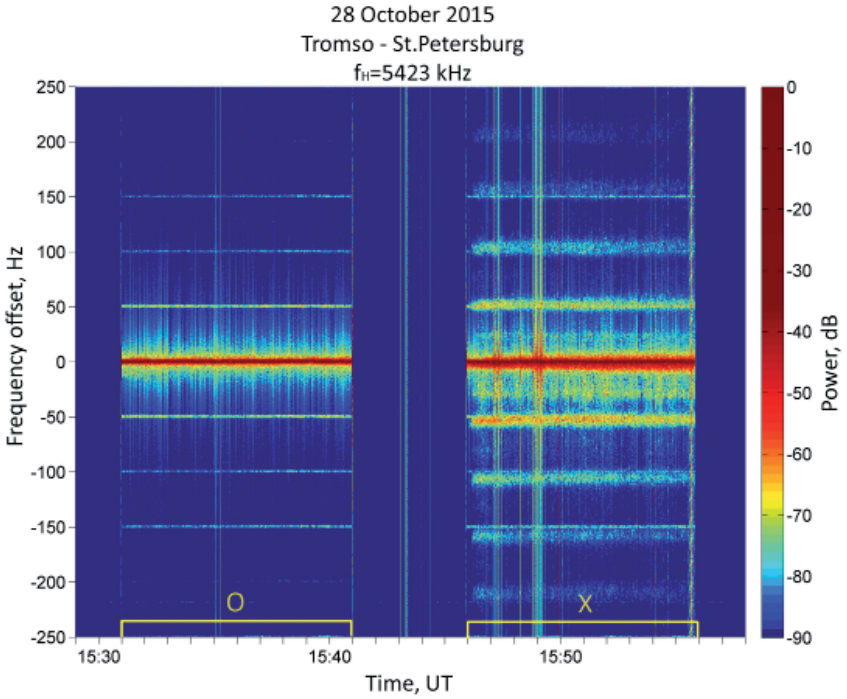

Figure 9. The spectrogram of the narrowband stimulated electromagnetic emission structures recorded at a distance of about 1200 km away from the EISCAT heater for alternating O/X-mode HF pumping towards the magnetic zenith at $f_H = 5.423$ MHz with an effective radiated power of 238 MW on 28 October 2015.

as the immediate response to the onset of the O-mode HF pumping, had a threshold of 0.17 V/m [48], which was much less the excitation threshold of persistent O-mode plasma and ion lines due to the non-resonance instability (0.62 V/m).

7. Narrowband Stimulated Electromagnetic Emission (NSEE)

Recent experiments at EISCAT have demonstrated that an X-mode HF pump wave is capable of exciting various discrete structures in the narrowband stimulated electromagnetic emission (NSEE) spectra (within ±1 kHz of the pump frequency) recorded at 1200 km away from the heating facility [35, 36, 49]. Figure 9 illustrates the spectrogram of the narrowband stimulated electromagnetic emission structures recorded at a distance about 1200 km away from the EISCAT heater for alternating O/X-mode HF pumping at $f_H = 5.423$ MHz on 28 October 2015. An X-mode pump wave reflected at an altitude of about 220 km. In accordance with the IGRF model at an altitude of 220 km, the values of the electron, f_{ce}, and ion (for O^+ ions), f_{ci}, gyro-frequencies were 1.364 MHz and 46.8 Hz, respectively. The pump frequency was thus 33 kHz below $4f_{ce} = 5.456$ MHz.

As seen from Figure 9, only during the X-mode cycle the down and upshifted (relative to the pump frequency) discrete spectral structures (Stokes and anti-Stokes modes), ordered by the ion gyro-frequency (for O^+ ions), were generated. Together with the spectral lines with the maxima at nf_{ci}, where n is the number of the ion gyro-harmonic, the downshifted and occasionally even upshifted spectral components at $0.5f_{ci}$ were also generated. In the course of the O-mode cycle, the discrete spectral structures were not recorded. Only very weak and narrow power-supply harmonic interference at multiples of 50 Hz can be seen during the O-mode transmission pulse.

We provided the first experimental evidence of the sensitivity of phenomena induced by the X-mode HF high-power radio waves to pump frequency stepping through the fifth electron gyro-harmonic ($5f_{ce}$) from below to above [49]. Figure 10 shows the spectrograms of the HF pump wave within a ±250 Hz band taken in the vicinity of St. Petersburg in the course of pump frequency stepping through the fifth electron gyro-harmonic for alternating O-mode and X-mode heating at Tromsø on 25 and 26 October 2013 [49]. The data were obtained with a frequency resolution of 0.2 Hz and a time resolution of 5 s. The strong line in the center with zero frequency offset corresponds to the pump wave frequency. The narrowband stimulated electromagnetic emission band on the spectrograms is represented in such a way that the maximum in the spectrum is at the pump frequency. As evident from Figure 10, during the O-mode pump pulse there were not any spectral structures in the spectrograms. In contrast, X-mode pulses exhibited a wide variety of spectral components.

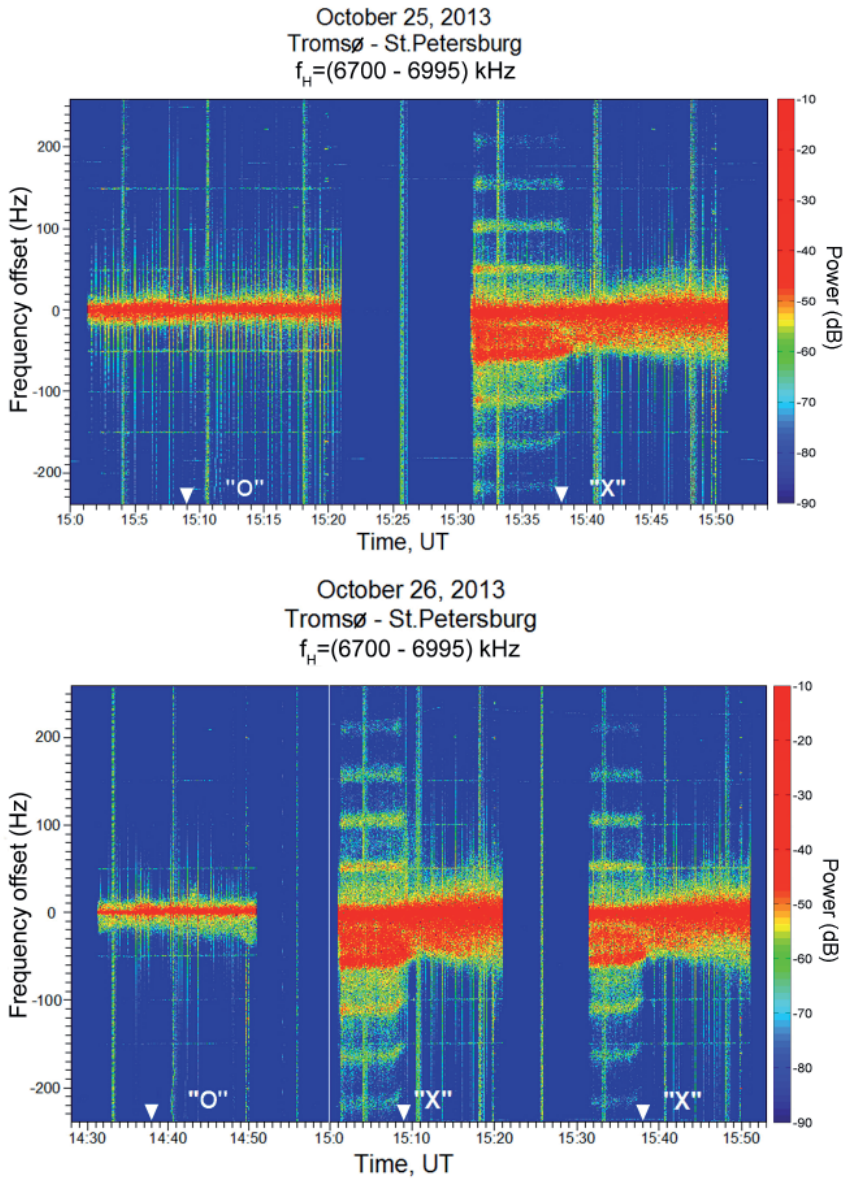

Figure 10. The spectrogram of the narrowband stimulated electromagnetic emission structures recorded with a frequency resolution of 0.2 Hz and a time resolution of 5 s at a distance of 1200 km from EISCAT/heating for alternating O/X-mode HF pumping towards the magnetic zenith on 25 and 26 October 2013 in the course of pump frequency stepping from 6.7 MHz to 6.995 MHz by 5 kHz steps every 20 s across the fifth electron gyro-harmonic. The effective radiated power varied between 657 MW to 715 MW and 456 MW to 501 MW in different transmission pulses. The strong line in the center with zero frequency offset was the pump wave. The narrowband stimulated electromagnetic emission band is represented in such a way that the maximum in the spectrum at the pump frequency corresponded to zero frequency offset at any time. Arrows indicate the time when $f_H = 5f_{ce}$ (adapted from Blagoveshchenskaya et al. [49]).

At pump frequencies $f_H < 5f_{ce}$, the narrowband stimulated electromagnetic emission spectra exhibited very intense downshifted and upshifted discrete structures ordered by the ion gyro-frequency (for O^+ ions). They are similar to the discrete spectral components observed below $4f_{ce}$ (see Figure 9). As the pump frequency reached $5f_{ce}$, discrete spectral lines were greatly suppressed and disappeared in the vicinity of $5f_{ce}$ and did not reappear at $f_H > 5f_{ce}$ [49].

It is suggested that the spectral structures observed below $4f_{ce}$ and $5f_{ce}$ are related to the magnetized stimulated Brillouin scatter (MSBS) process, when the HF pump wave directly decays into the ion gyro-harmonic and a backscattered electromagnetic wave. Artificial field-aligned irregularities play a key role for the narrowband stimulated electromagnetic emission occurrence at a large distance from the EISCAT/Heating. Backscattered EM waves, generated due to the magnetized stimulated Brillouin scatter process, are scattered from artificial field-aligned irregularities and are capable of propagating to a large distance from the heating facility without significant attenuation.

8. Concluding Remarks

In the last 50 years, most HF pumping experiments in the upper ionosphere (*F* region) at different ground-based HF heating facilities in the world were carried out with the use of ordinary polarized (O-mode) powerful HF radio waves. We have presented the first experimental evidence showing that extraordinary (X-mode) powerful HF radio waves, injected into the high-latitude ionospheric F2 layer towards the magnetic zenith, are capable of generating artificial field-aligned irregularities, radio-induced optical emissions at red (630 nm) and green (557.7 nm) lines, strong electron acceleration leading to N_e enhancements, ion-acoustic and Langmuir electrostatic waves, and spectral components in the narrowband stimulated electromagnetic emission spectra observed at a large distance from the HF heater. The results obtained were briefly reported in Sections 3 through 7.

In spite of the fact that the excitation of various unexpectedly strong X-mode phenomena in the F region of the high-latitude ionosphere is a repeatable and easily reproducible feature from EISCAT heating experiments, many aspects of the nonlinear interaction between an X-polarized HF pump wave and the ionospheric plasma still remain poorly understood. Up to the present, an adequate theory describing the interactions between the X-mode HF pump wave and ionospheric plasma is absent. Further clarification and theoretical background are needed to explain the origin of unusually strong phenomena excited in the ionospheric *F*-region by X-polarized HF pump waves.

Langmuir and ion-acoustic turbulence, seen as HF-enhanced ion and plasma lines (HFIL and HFPL) in the incoherent radar spectra, are indicative of the parametric decay instability (PDI). However, it is not clear through what mechanism an X-mode pump wave can excite the parametric decay instability and even the modulational instability (MI), especially taking into account that the X-mode HF-enhanced ion line and HF-enhanced plasma line are of much higher intensity, as compared with the O-mode effects, and were observed throughout the whole HF pump pulse and coexist with strong artificial small-scale field-aligned irregularities.

Strong N_e enhancements from EISCAT UHF radar measurements are typical for X-mode pumping and observed as often as the T_e enhancements under the action of O-polarized HF pump waves. They occurred along the magnetic field line in a wide altitude range, whether or not the HF-enhanced ion and plasma lines were excited. The origin of such N_e enhancements under X-mode HF pumping is not yet fully understood and needs clarification. In principle, the accelerated electrons can produce the enhanced ionization. Hence, an efficient mechanism of the electron acceleration induced by an X-polarized pump wave should be found.

The generation mechanisms of narrowband discrete spectral structures observed under X-mode HF pumping at a large distance from an HF heating facility are not clearly understood and require a solid theoretical basis.

The new EISCAT_3D radar [50] planned to run in 2022 will provide unprecedented temporal and spatial resolution measurements with an extended coverage in height and horizontal extent of the heated volume. It can provide the detailed investigations of the various X-mode phenomena occurring in the magnetic field-aligned direction, including large-scale and small-scale field-aligned irregularities, Langmuir and ion-acoustic plasma waves with high temporal and spatial resolution, and N_e enhancements due to the acceleration of electrons. However, the location of the existing EISCAT HF heating facility cannot provide field-aligned measurements with the use of the EISCAT_3D radar. A new HF heating facility, located in close proximity to the EISCAT_3D site, is needed to realize the three-dimensional capabilities of the new radar. The combination of the EISCAT_3D radar with a new HF heating facility will provide answers to many outstanding scientific questions related to the nonlinear interaction between powerful electromagnetic waves and the high-latitude ionospheric plasma.

9. Acknowledgements

EISCAT is an international scientific association supported by research organizations in China (CRIRP), Finland (SA), Japan (NIPR and STEL), Norway (NFR), Sweden (VR), and the United Kingdom (NERC). The author is thankful to members of her team, especially Dr. T. D. Borisova, Dr. A. S. Kalishin, V. A. Kornienko, and D. D. Rogov. She is also grateful to colleagues with whom she collaborated in the past or is collaborating with in the present time, namely Prof. Bo Thidé, Prof. A. Brekke, Prof. T. Yeoman, Dr. M. Kosch, Dr. I. Häggström, Dr. M. Rietveld, and Dr. U. Brändsröm. The author thanks Prof. A. Pellinen-Wannberg for valuable discussions.

10. References

1. N. F. Blagoveshchenskaya, V. A. Kornienko, T. D. Borisova, B. Thidé, M. J. Kosch, M. T. Rietveld, E. V. Mishin, R. Y. Luk'yanova, and O. A. Troschichev, "Ionospheric HF Pump Wave Triggering of Local Auroral Activation," *Journal of Geophysical Research*, **106**, A12, 2001, pp. 29071-29090.

2. N. F. Blagoveshchenskaya, V. A. Kornienko, T. D. Borisova, M. T. Rietveld, T. Bösinger, B. Thidé, T. B. Leyser, and A. Brekke," Heater-Induced Phenomena in a Coupled Ionosphere-Magnetosphere System," *Advances of Space Research*, **38**, 2006, pp. 2495-2502, https://doi.org/10.1016/j.asr.2004.12.047.

3. N. F. Blagoveshchenskaya, T. D. Borisova, V. A. Kornienko, B. Thidé, M. T. Rietveld, M. J. Kosch, and T. Bösinger, "Phenomena in the Ionosphere – Magnetosphere System Induced by Injection of Powerful HF Radio Waves into Nightside Auroral Ionosphere," *Annales Geophysicae*, **23**, 2005, pp. 87-100.

4. V. A. Kornienko, N. F. Blagoveshchenskaya, T. D. Borisova, B. Thidé, and A. Brekke, "Modification of the Local Substorm Ionospheric and Field-Aligned Currents Produced by the Tromsø Heating Facility," *International Journal of Geomagnetism and Aeronomy*, **4**, 1, 2003, pp. 37-46.

5. N. F. Blagoveshchenskaya, *Geophysical Effects of Active Impacts in Near-Earth Space* (in Russian), St. Petersburg, Gidrometeoizdat, 2001.

6. T. D. Borisova, N. F. Blagoveshchenskaya, V. A. Kornienko, M. T. Rietveld, B. Thidé, and T. B. Leyser, "Ionospheric Effects Observed when the Tromsø HF Heating Facility Was Turned On/Off," *Geomagnetism and Aeronomy*, **45**, 3, 2005, pp. 367-374.

7. M. T. Rietveld, M. J. Kosch, N. F. Blagoveshchenskaya, V. A. Kornienko, T. B. Leyser, and T. K. Yeoman, "Ionospheric Electron Heating, Aurora and Striations Induced by Powerful HF Radio Waves at High Latitudes: Aspect Angle Dependence," *Journal of Geophysical Research*, **108**, A4, 2003, 1141, doi:10.1029/2002 JA 009543.

8. M. J. Kosch, H. Vickers, Y. Ogawa, A. Senior, and N. Blagoveshchenskaya, "First Observation of the Anomalous Electric Field in the Topside Ionosphere by Ionospheric Modification over EISCAT," *Geophysical Research Letters*, **41**, 2014, doi:10.1002/2014GL061679.

9. N. F. Blagoveshchenskaya, V. A. Kornienko, A. V. Petlenko, A. Brekke, and M. T. Rietveld, "Geophysical Phenomena During an Ionospheric Modification Experiment at Tromsø," *Annales Geophysicae*, **16**, 1998, pp. 1212-1225.

10. T. D. Borisova, N. F. Blagoveshchenskaya, V. A. Kornienko, and M. Rietveld, "Characteristics of *Pc*4-5 Pulsations Obtained by the HF Radio Wave Bi-Static Backscatter Method Using the HF EISCAT/Heating Facility and Ground Magnetometers," *Geomagnetism and Aeronomy*, **51**, 4, 2011, pp. 630-642.

11. T. D. Borisova, N. F. Blagoveshchenskaya, I. M. Ivanova, and M. T. Rietveld, "Dependence of the *Pc*4 Magnetic Pulsation Parameters on the Radiated Power of the EISCAT HF Heating Facility," *Geomagnetism and Aeronomy*, 53, 1, 2013, pp. 32-42, doi:10.1134/S0016793213010040.

12. N. F. Blagoveshchenskaya, V. A. Kornienko, T. D. Borisova, I. V. Moskvin, M. T. Rietveld, V. L. Frolov, V. P. Uryadov, L. M. Kagan, Yu. M. Yampolski, V. L. Galushko, A. V. Koloskov, S. B. Kasheev, A. V. Zalizovski, G. G. Vertogradov, V. G. Vertogradov, and M. C. Kelley, "Probing of Medium-Scale Traveling Ionospheric Disturbances Using HF-Induced Scatter Targets," *Annales Geophysicae*, **24**, 2006, pp. 2333-2345.

13. T. R. Robinson, "The Heating of the High Latitude Ionosphere by High Power Radio Waves," *Physics Reports*, **179**, 1989, pp.79-209.

14. A. V. Gurevich, "Nonlinear Effects in the Ionosphere," *Physics-Uspekhi*, **50**, 2007, pp. 1091-1121.

15. A. V. Streltsov, et al., "Past, Present and Future of Active Radio Frequency Experiments in Space," *Space Science Review*, **214**, 118, 2018, https://doi.org/10.1007/s11214-018-0549-7.

16. N. F. Blagoveshchenskaya, V. A. Kornienko, M. T. Rietveld, B. Thidé, A. Brekke, I. V. Moskvin, and S. Nozdrachev, "Stimulated Emissions Around the Second Harmonic of Tromsø Heater Frequency Observed by Long-Distance Diagnostic HF Tools," *Geophysical Research Letters*, **25**, 1998, pp. 873-876.

17. N. F. Blagoveshchenskaya, T. D. Borisova, V. A. Kornienko, T. B. Leyser, M.T. Rietveld, and B. Thidé, "Artificial Field-Aligned Irregularities in Night-Side Auroral Ionosphere," *Advances in Space Research*, **38**, 2006, pp. 2503-2510.

18. N. F. Blagoveshchenskaya, V. A. Kornienko, A. Brekke, M. T. Rietveld, M.J Kosch, T. D. Borisova, and M. V. Krylosov, "Phenomena Observed by HF Long-Distance Tools in the HF Modified Auroral Ionosphere During Magnetospheric Substorm," *Radio Science*, **34**, 1999, pp. 715-724.

19. T. D. Borisova, N. F. Blagoveshchenskaya, I. V. Moskvin, M. T. Rietveld, M. J. Kosch, and B. Thidé, "Doppler Shift Simulation of Scattered HF Signals During the Tromsø HF Pumping Experiment on 16 February, 1996," *Annales Geophysicae*, **20**, 2002, pp. 1479-1486.

20. N. F. Blagoveshchenskaya, H. C. Carlson, V. A. Kornienko, T. D. Borisova, M. T. Rietveld, T. K. Yeoman, and A. Brekke, "Phenomena Induced by Powerful HF Pumping Towards Magnetic Zenith with a Frequency Near the *F*-region Critical Frequency and the Third Electron Gyro Harmonic Frequency," *Annales Geophysicae*, **27**, 2009, pp. 131-145.

21. N. F. Blagoveshchenskaya, T. D. Borisova, T. K. Yeoman, and M. T. Rietveld, "The Effects of Modification of a High-Latitude Ionosphere by High-Power HF Radio Waves. Part 1. Results of Multi-Instrument Ground-Based Observations," *Radiophysics and Quantum Electronics*, **53**, 2011, pp. 512-531.

22. T. D. Borisova, N. F. Blagoveshchenskaya, A. S. Kalishin, M. J. Kosch, A. Senior, M. T. Rietveld, T. K. Yeoman, and I. Hägström, "Phenomena in the High-Latitude Ionospheric *F* Region Induced by a HF Heater Wave at Frequencies Near the Fourth Electron Gyroharmonic," *Radiophysics and Quantum Electronics*, **57**, 2014, pp. 1-19.

23. T. D. Borisova, N. F. Blagoveshchenskaya, A. S. Kalishin, M. T. Rietveld, T. K. Yeoman, and I. Hägström, "Modification of the High-Latitude Ionospheric *F* Region by High-Power HF Radio Waves at Frequencies Near the Fifth and Sixth Electron Gyroharmonics," *Radiophysics and Quantum Electronics*, **58**, 2016, pp. 561-585.

24. T. D. Borisova, N. F. Blagoveshchenskaya, M. T. Rietveld, and I. Häggström, "Outshifted Plasma Lines Observed in Heating Experiments in the High-Latitude Ionosphere at Pump Frequencies Near Electron Gyroharmonic," *Radiophysics and Quantum Electronics*, **61**, 10, 2019, pp. 722-740.

25. M. T. Rietveld, A. Senior, J. Markkanen, and A. Westman, "New Capabilities of the Upgraded EISCAT High-Power HF Facility," *Radio Science*, **51**, 9, 2016, pp. 1533-1546, doi:10.1002/2016RS006093.

26. H. Rishbeth and T. van Eyken, "EISCAT: Early History and the First Ten Years of Operation," *Journal of Atmospheric and Solar-Terrestrial Physics*, **55**, 1993, pp. 525-542.

27. M. Lester, et al., "Stereo CUTLASS: A New Capability for the SuperDARN Radars," *Annales Geophysicae*, **22**, 2004, pp. 459-473.

28. U. Brändström, *The Auroral Large Imaging System – Design, Operation and Scientific Results*, PhD thesis, Swedish Institute of Space Physics, Kiruna, Sweden, October 2003 (IRF Scientific Report 279), ISBN: 91-7305-405-4.

29. N. F. Blagoveshchenskaya, T. D. Borisova, V. A. Kornienko, V. L. Frolov, M. T. Rietveld, and A. Brekke, "Some Distinctive Features in the Behavior of Small-Scale Artificial Ionospheric Irregularities at Mid- and High Latitudes," *Radiophysics and Quantum Electronics*, **50**, 8, 2007, pp. 619-632.

30. D. D. Rogov, N. F. Blagoveshchenskaya, and T. K. Yeoman, "Features of Artificial Ionospheric Irregularities Induced by Powerful HF Radio Waves from Bi-Static Scatter Measurements," Conference Radiation and Scattering of Electromagnetic Waves (RSEMW) 2019, doi:10.1109/RSEMW.2019.8792727.

31. N. F. Blagoveshchenskaya, T. D. Borisova, T. Yeoman, M. T. Rietveld, I. M. Ivanova, and L. J. Baddeley, "Artificial Field-Aligned Irregularities in the High-Latitude *F* Region of the Ionosphere Induced by an X-mode HF Heater Wave," *Geophysical Research Letters*, **38**, 2011, L08802, doi: 10.1029/2011GL046724.

32. N. F. Blagoveshchenskaya, T. D. Borisova, M. T. Rietveld, T. K. Yeoman, D. M. Wright, M. Rother, H. Luhr, E. V. Mishin, and C. Roth, "Results of Russian Experiments Dealing with the Impact of Powerful HF Radiowaves on the High Latitude Ionosphere Using the EISCAT Facilities," *Geomagnetism and Aeronomy*, **51**, 8, 2011, pp. 1109-1120.

33. N. F. Blagoveshchenskaya, T. D. Borisova, T. K. Yeoman, M. T. Rietveld, I. Häggström, and I. M. Ivanova, "Plasma Modifications Induced by an X-mode HF Heater Wave in the High Latitude *F* Region of the Ionosphere," *Journal of Atmospheric and Solar-Terrestrial Physics*, **105-106**, 2013, pp. 231-244.

34. N. F. Blagoveshchenskaya, T. D. Borisova, M. Kosch, T. Sergienko, U. Brändström, T. K. Yeoman, and I. Häggström, "Optical and Ionospheric Phenomena at EISCAT Under Continuous X-Mode HF Pumping," *Journal of Geophysical Research: Space Physics*, **119**, 2014, pp. 10,483-10,498, doi:10.1002/ 2014JA020658.

35. N. F. Blagoveshchenskaya, T. D. Borisova, T. K. Yeoman, I. Häggström, and A. S. Kalishin, "Modification of the High Latitude Ionosphere *F* Region by X-Mode Powerful HF Radio Waves: Experimental Results from Multi-Instrument Diagnostics," *Journal of Atmospheric and Solar-Terrestrial Physics*, **135**, 2015, pp. 50-63, https://doi.org/10.1016/j.jastp.2015.10009.

36. N. F. Blagoveshchenskaya, T. D. Borisova, A. S. Kalishin, V. N. Kayatkin, T. K. Yeoman, and I. Häggström, "Comparison of the Effects Induced by the Ordinary (O-Mode) and Extraordinary (X-Mode) Polarized Powerful HF Radio Waves in the High-Latitude Ionospheric *F* Region," *Cosmic Research*, **56**, 1, 2018, pp. 11-25.

37. N. F. Blagoveshchenskaya, T. D. Borisova, A. S. Kalishin, T. K. Yeoman, Yu. A. Schmelev, and E. E. Leonenko, "Characterization of Artificial, Small-Scale,

Ionospheric Irregularities in the High-Latitude *F* Region Induced by High-Power, High-Frequency Radio Waves of Extraordinary Polarization," *Geomagnetism and Aeronomy*, **59**, 6, 2019, pp.759-773.

38. N. Borisov, F. Honary, and H. Li, Excitation of Plasma Irregularities in the *F*-Region of the Ionosphere by Powerful HF Radio Waves of X-polarization, *Journal of Geophysical Research: Space Physics*, **123**, 2018, pp.5246-5260, doi.org/10.1029/2018JA025530.

39. S. Kuo, "Ionospheric Modifications in High Frequency Heating Experiments," *Physics Plasmas*, **22**, 2015, 012901, doi: 10.1063/1.4905519.

40. M. J. Kosch, Y. Ogawa, M. T. Rietveld, S. Nozawa, and R. Fujii, "An Analysis of Pump-Induced Artificial Ionospheric Ion Upwelling at EISCAT," *Journal of Geophysical Research*, **115**, 2010, A12317, doi:10.1029/2010JA015854.

41. N. F. Blagoveshchenskaya, T. D. Borisova, A. S. Kalishin, T. K. Yeoman, and I. Häggström, "Distinctive Features of Langmuir and Ion-Acoustic Turbulences Induced by O- and X-Mode HF Pumping at EISCAT," *Journal of Geophysical Research: Space Physics*, **125**, 2020, doi: 10.1029/2020JA028203.

42. M. T. Rietveld and A. Senior, "Ducting of Incoherent Scatter Radio Waves by Field-Aligned Irregularities," *Annales Geophysicae*, 2020, in press, doi: 105194/angeo-2020-22.

43. H. C. Carlson, V. B., Wickwar, and G. P. Mantas, "Observations of Fluxes of Suprathermal Electrons Accelerated by HF excited Instabilities," *Journal of Atmospheric and Solar-Terrestrial Physics*, **44**, 1982, pp. 1089-1100.

44. T. Hagfors, W. Kofman, H. Kopka, P. Stubbe, and T. Äijänen, "Observations of Enhanced Plasma Lines by EISCAT During Heating Experiments," *Radio Science*, **18**, 1983, pp. 861-866.

45. P. Stubbe, H. Kohl, and M. T. Rietveld, "Langmuir Turbulence and Ionospheric Modification," *Journal of Geophysical Research*, **97**, 1992, pp. 6285-6297.

46. N. F. Blagoveshchenskaya, T. D. Borisova, and T. K. Yeoman (2017), "Comment on the Article 'Parametric Instability Induced by X-Mode Wave Heating at EISCAT' by Wang et al. (2016)," *Journal of Geophysical Research: Space Physics*, **122**, 2017, pp. 12,570-12,586, https://doi.org/10.1002/2017JA023880.

47. T. D. Borisova, N. F. Blagoveshchenskaya, T. K. Yeoman, and I. Häggström, "Excitation of Artificial Ionospheric Turbulence in the High-Latitude Ionospheric *F* Region as a Function of the EISCAT/Heating Effective Radiated Power," *Radiophysics and Quantum Electronics*, **60**, 4, 2017, https://doi.org/10.1007/s11141-017-9798-7.

48. C. Bryers, M. Kosch, A. Senior, M. T. Rietveld, and T. K. Yeoman, "The Thresholds of Ionospheric Plasma Instabilities Pumped by High-Frequency Radio Waves at EISCAT," *Journal of Geophysical Research: Space Physics*, **118**, 2013, pp. 7472-7481.

49. N. F. Blagoveshchenskaya, T. D. Borisova, A. S. Kalishin, T. K. Yeoman, and I. Häggström, "First Observations of Electron Gyro-Harmonic Effects Under X-Mode HF Pumping the High Latitude Ionospheric *F*-Region," *Journal of Atmospheric and Solar-Terrestrial Physics*, **155**, 2017, pp. 36-49, doi:10.1016/j.jastp.2017.02.003.

50. I. McCrea, A. Aikio, L. Alfonsi, E. Belova, S. Buchert, M. Clilverd, N. Engler, B. Gustavsson, C. Heinselman, J. Kero, M. Kosch, H. Lamy, T. Leyser, Y. Ogawa, K. Oksavik, A. Pellinen-Wannberg, F. Pitout, M. Rapp, I. Stanislawska, and J. Vierinen, "The Science Case for the EISCAT_3D Radar," *Progress in Earth and Planetary Science*, **2**, 2015, https://doi.org/10.1186/s40645-015-0051-8.